IMT Estimation through Points of Interest based on Surf and MSER Descriptors

Tareeq Zaid[1], Nagashettappa Biradar[2] and Mahesh V Sonth[3]

Department of Electronics and Communication Engineering

Bheemanna Khandre Institute of Technology Bhalki, India[1, 2], CMR Technical Campus Hyderabad, India[3]

E-mail:- *tareeq.vlsi@gmail.com[1], nmbiradar@gmail.com[2], maheshsonth@gmail.com[3]*

DOI: - https://doi.org/10.47531/MANTECH/ECC.2021.33

Abstract

One of the essential variables in approving the cardio vascular malady is through the estimation of intima media thickness (IMT) from ultrasound imaging. Impediments in evaluating the IMT are fundamentally worried about heterogeneous force varieties for various tissues. In this paper, a focal point based element descriptor for the most part SURF and MESH procedures are executed which is approved with the IMT thickness assessed therein. Exploratory outcomes show improved execution with mean squared error of than 16.0 in SURF when contrasted with MESH based descriptor.

Keywords: - *Ultrasound imaging, Intima Media Thickness, SURF, MSER.*

INTRODUCTION

Atherosclerosis is analyzed through the assessment of the harming variables of the uncovered endothelium, therefore brought sores up in vessel divider and atherosclerotic plaque happen. Making forecast in a beginning phase of such a condition is testing, in this manner non-obtrusive proxy markers were created to recognize various phases of cardiovascular malady. The administration and following of atherosclerosis is additionally performed through estimating the Intima-Media Thickness (IMT). The Intima-Media complex speaks to the internal layers of the vascular layers after the endothelial inward layer which connotes the movement of infection developing from that region.

Subsequently, the utilization of b-mode ultrasound imaging in estimating the intima-media thickness has become a predominant strategy in diagnosing atherosclerotic disease [1]– [4]. Be that as it may, the vast majority of the strategies associated with estimating the IMT included manual distinguishing proof of reverberation facilitates at discrete focuses. This endured confinement chiefly due to interobserver fluctuation and picture goal. This lead to improvement of mechanized division of IMT in ultrasound pictures. A portion of the procedures utilized include edge following and slope based strategies, dynamic programming, dynamic shapes, neighborhood insights, Nakagami displaying and Hough based changes [5], [6].

Be that as it may, the exhibition of these procedures relies upon different variables including natural changeability, instrumental fluctuation and clamor sources. For example, the nearness of plaque is recognized as an infringement into the blood vessel lumen of atleast half of the encompassing IMT esteem with a thickness of more prominent than 1.5 mm, this progressions the presence of the carotid course in the ultrasound imaging [7], such causes decrease the exhibition of the division strategies as they intensely depend on the morphology and the presence of the carotid vein. These division procedures are additionally seen to be successful just in client subordinate structures, for example the power scope of course lumen and adventitia are 0-5 and 180-190 individually for a 8 piece picture, anyway this shifts when goal of the picture is changed in an alternate scanner, making manual intercession vital.

The paper is organized as follows, Section II involves reviewing the literature of limitations to ultrasound imaging and its effects on the segmentation techniques. Section III describes the proposed methodology and implementation details. Section IV explains the obtained results and analysis followed by conclusion and future scope.

REVIEW OF LITERATURE

In this section, different techniques pertaining to the segmentationc of the carotid wall is described,

along with their prevalent issues and limitations. Initial techniques pertaining to the carotid wall segmentation were based on detecting the edges. Pignoli and Longo [8] first proposed computational methods in aiding the IMT measurement. It mainly involved intensity profiling from center of the vessels to the border. The adventitia layers were clearly identifiable along with lumen of the artery. Further, Ligouri et. al [9], proposed a segmentation technique which was based on image gradients. A horizontally placed B-mode image was considered for this technique. An ideal gradient is identified to have dark pixels for the artery lumen and the origination of the carotid walls occur from the gradient transitions. However, given the noise measured intensity gradient is different in experiments as compared to theoretical values. As compared to previous studies, Ligouri et. al considered statistical thresholding for reducing noise before image gradient computation. However, this technique had the limitation of semi automation.

Stein et. al [10] proposed a gradient based technique on estimating the IMT of the carotid distal wall. The technique was mainly introduced for the purpose of testing the computer based methods on vessel wall segmentation. The experiment resulted in measuring error in IMT measurement at 12.0±6.0 μm. Noise characteristics were not considered during this experiment.

Faita et. al [11] proposed another gradient based edge based segmentation. The technique mainly involves First Order Absolute Moment Edge Operator (FOAM) along with a pattern recognition approach. The overall performance of the technique had significantly shown improvement as compared to previous segmentation techniques. The error measurement for IMT estimation was 10.0±38.0 μm. Main significance of this technique is its real time applicability in clinical setting. However, such a technique is limited in its approach when considering curved vessels. Other methods mainly involving dynamic programming techniques addressed the variability in ultrasound imaging caused during manual measurements.

Wendelhag et. al [12] introduced first dynamic programming techniques to automate detection of echo interfaces. The factors involved in this techniques were echo intensity, intensity gradient and boundary continuity. The error measurement of the IMT was 40±36 μm. The advantage of considering such a computational method reduced the difference in segmenting of differently trained operators. However, a major limitation in this technique was it is scanner dependent, i.e. the obtained cost function of the features was highly dependent on noise characteristics.

A similar kind of study was performed by Liang et. al [13] in 2000 based on a multiscale analysis. A two level dynamic programming approach was applied for involving indicating the global position of the artery in an image (coarser scale) and wall layers estimated at a finer scale. This improved technique reduced the computational complexity as compared to previous dynamic programming technique. The error estimation of the IMT was calculated to be 42.0±20.0μm.

Gutierrez et. al [14] proposed a technique based on active contours and multiresolution methods to automate carotid IMT and lumen diameter estimation. Further each wall of the active contours were modeled using active contours Lobregt and Virgever et. al [15]. The overall error estimation of the IMT was 90.0±60.0 μm. This technique mainly used the damping force which helped in smoothing and stabilizing contour evolution.

Another major issue concerning the snakes model was that of the methods of image quality assessments. A summarized study was conducted by Loizou et. al [16] to address problems pertaining to image preprocessing, standardization, noise characteristics and tuning of parameters of snakes model. Further development in the snakes model were proposed involving the concept of local statistics.

Recent advances in the field of machine learning techniques have enabled robust and efficient developments in full automated segmentation of the carotid artery. The experimental result is compared with manual tracings with respect to the overall accuracy of the proposed technique. The advantages of CCA segmentation using machine learning among other factors is in its computational efficiency. Other methods in CCA segmentation involve fuzzy c-means, RBF, etc [17].

METHODOLOGY

The proposed method intends to fully automate the IMT Segmetnation through homogenous pixel charecteristics obtained from the point of interest image descriptors. The resulting segmentation technique significantly reduces manual intervention which is a crucial application in remote sensing application in medical imaging. Segmentation of the CCA for IMT estimation and validating the same is performed in 3 stages [18] which involves image preprocessing, feature

extraction, model selection and validation shown in Fig. 1.

A. Dataset Description and image preprocessing

An open source dataset [19] was considered for this experiment. This dataset contained CCA ultrasound images of 10 volunteers with mean age of 27.5_3.5 years and mean weight of 76.5±9.7 kg. The images were captured in patients lying in supine position with neck rotated to left side during examination of the right CCA. A Sonix OP ultrasound scanner was used for data acquisition with variable parameters of setup depth, gain, time gain compensation (TGC) curve and different linear array transducers. The resulting image resolution is 390 x 330 px. Due to susceptibility factors involved in the imaging of the superficial organs, two linear array transducers with 10Mhz and 14Mhz were used. The scanning of these arteries were performed by specialist with more than 5 years of experience. In this experiment, a total of 84 samples are considered.

A Gaussian based noise characteristics are applied to the raw image with constant mean and variance with 0 and 0.01 respectively. An averaging filter is used as a denoising technique [20]. A limitation in ultrasound imaging is that processing and analysis of visual and structural aspects in imaging is difficult, which necssitiates the application of image smoothening. For this purpose, an averaging filter smoothens the image for a clearer view of the structure of the pathology through imaging.

B. Snakes based segmentation model – Dual Line Detection

A gradient magnitude in the form of edge map is defined which refers the boundary of the object to be segmented as shown in Fig. 2. Based on this edge map, an LDLD technique

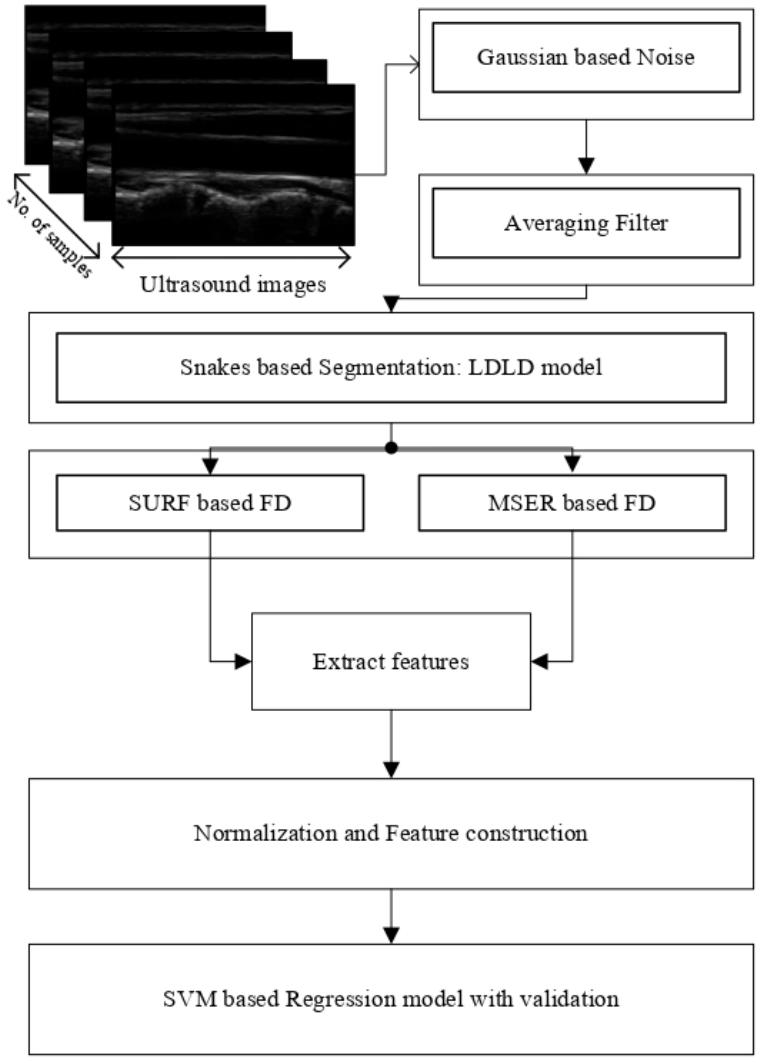

Fig. 1: Block diagram of the proposed CCA segmentation model

Is applied which initializes approximation to the boundary. As a result number of image segments is calculated given as:

$$S = \frac{N}{I_{MAX}} \quad (1)$$

Where IMAX! Maximum width a segment can achieve.

Further, an independent normalization is performed for each segment which is threshold by a global constant to identify local edge points. Due to the inaccuracies of initial contours, a snakes based model is implemented for segmentation. This results in deriving the LI contour and MA contours for CCA segmentation. The distance between these contours isv measured and is considered as the target variable (reference variable) in the SVM based regression model later in this experiment.

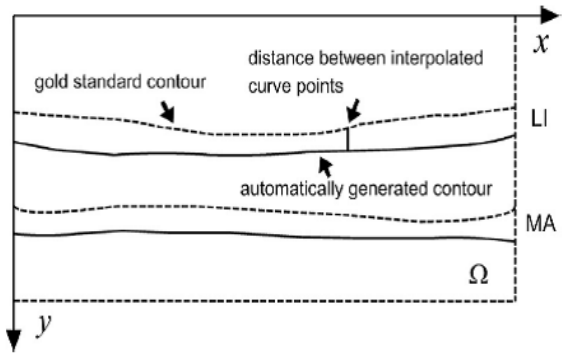

Fig. 2: Defined segmentation error of LI, MA and IMC

C. Image feature descriptors for CCA segmentation and identification

Imaging features are obtained through points of interest based techniques mainly SURF (Speeded Up Robust Features) and MSER (Maximally Stable External Regions). In any methods pertaining to the points based image description, three steps are involved, first interest points such as corners, blobs and T-junctions are selected which are distinctively located in an image. These descriptors are selected which often times are found to be repeated in an image. Secondly, neighborhood of every interest points is presented as a feature vector. Finally, descriptor vectors are matched between different images based on certain distance vectors (Mahalanobis or Euclidean distance).

In order to detect points of interest using SURF based method, an approximation of the determinant of Hessian blob is performed, which can be further computed with 3 integer operations using a precomputed integral image. The resulting matrix is an N x 64 matrix, in which N represents each point of interest with 64 image descriptors. Another technique used in identifying the points of interest is the MSER (Maximally Stable External Regions), particularly used in detecting blobs. One of the primary advantages of the MSER is its exclusive definition of intensity function in region and outer border leading to key characteristics of regions. The resulting matrix is an N x 64, which N represents each points of interest with 64 image descriptors.

D. Featureset construction

The non-zero vectors of the matrix first identified and retained among the feature vectors from SURF and MSER based techniques. These non-zero vectors represent the valid image feature descriptors. Therefore, of the 84 samples, only 59 samples were considered for further analysis towards the Support Vector Machine (SVM) based regression model. Further, for every image sample, a set of vectors with 64 descriptors are computed individually for SURF and MSER based techniques. These individual vectors for every sample is computed for mean resulting in 1 x 64 vector for each image sample for individual feature descriptors.

RESULTS

The valuation of the proposed method involves three stages mainly at image quality assessment, consistency in estimating the IMT and performance of the regression model in validating the SURF and MSER based feature descriptors [21].

A. Image quality assessment

The quality of image after denoising process is assessed through the following metrics shown in Fig. 3, Signal to Noise Ratio (SNR): This measure is basically used to characterize the quality of the image. SNR is defined in terms of decibels of signal power in terms of noise power. It is defined as average signal value to the standard deviation of the signal,

$$SNR = \frac{\mu_{sig}}{\sigma_{sig}} \quad (2)$$

Peak Signal to Noise Ratio (PSNR): It is mostly defined through the mean squared error, given a noise free m x n image I and its approximation K, MSE can be defined as,

$$MSE = \frac{1}{mn}\sum_{i=0}^{m-1}\sum_{j=0}^{n-1}[I(i,j) - K(i,j)]^2 \quad (3)$$

$$PSNR = 20log_{10}(MAX_I) - 10log_{10}(MSE) \quad (4)$$

These metrics are calculated for all image samples for which descriptive statistics in terms of mean, median, minimum, maximum, etc are calculated which is shown in table X. As

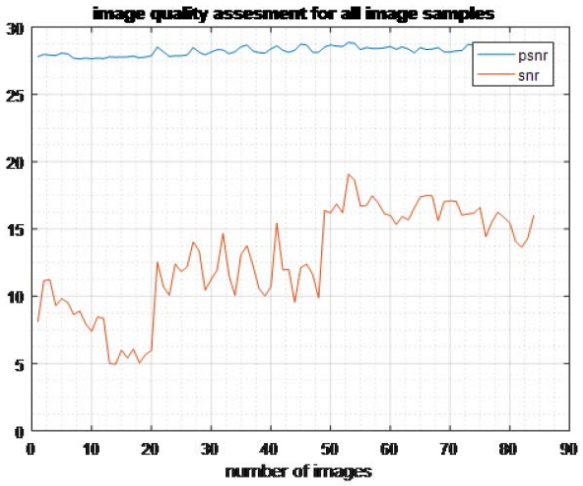

Fig. 3: Image quality assessment for all image samples

Table I: Descriptive statistics for image quality assessment

Measures	SNR	PSNR
Mean	12.76	28.23
Std. dev	3.7	0.32
Min.	4.94	27.64
Max.	19.08	28.87
Median	12.82	28.25

described in TABLE I, the assessment of the Gaussian noise in ultrasound imaging is filtered using averaging technique, As a result, the mean and standard deviation of the image samples SNR and PSNR are observed to be consistent. This makes it suitable for further processing to contour based technique for segmentation of the CCA model.

B. Validation of the IMT estimation

The IMT estimation is considered for all 84 image samples which is shown as in TABLE II, the contour based snakes model with LDLD based techniques has identified the IMT consistently throughout the image samples, with mean value of 26.68 and std deviation of 0.3157. Further, this estimation26.68 and std deviation of 0.3157. Further, this estimation

Table II: Descriptive statistics for IMT estimation

Parameter	mean	std. dev	median	min	max
IMT est.	26.68	0.3157	26.69	26.21	27.20

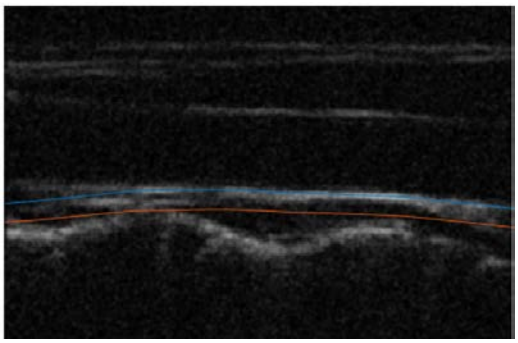

Fig. 4: IMT estimation of ultrasound images through contour based model

of the IMT is considered as a reference shown in Fig. 4 for constructing the regression based SVM model.

C. Validation of SURF and MSER based features through SVM regression model

The two feature descriptors considered in this experiment are the SURF and MSER based model, each method of feature descriptor consists of 64 feature descriptors for each point of interest. The feature descriptors for IMT estimation is given in Fig. 5. The mean across all points of interest for each of 64 descriptors is computed resulting in 1 x 64 for each sample.

The mean of all samples for each of 64 descriptors for the two techniques is shown in fig 8. A certain level of consistency is observed in both of the models (referred to both inter and intra modular similarities. An SVM based regression model is applied with an SMO based solver and a holdout of 0.1 of the entire dataset. The data is standardized before implementing the regression model. The model resulted in a mean squared error of 16.01 for SURF based feature descriptors and 80.97 for MSER based feature descriptors respectively. This indicates that SURF based features represent the IMT estimation more robustly than the MSER based technique shown in Fig. 6.

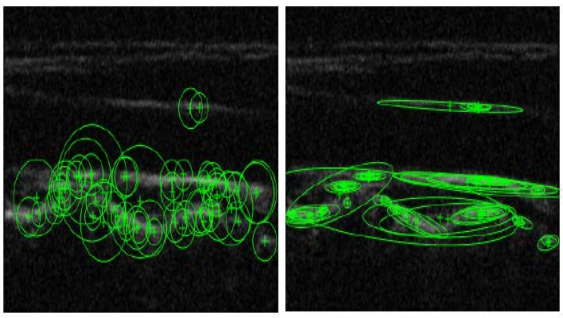

(a) SURF (b) MSER

Fig. 5: SURF and MSER based feature descriptors

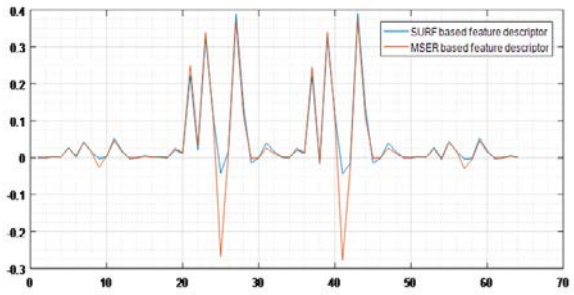

Fig. 6: Surf and MSER based feature descriptors (64 descriptors)

CONCLUSION

From the conducted study, a robust estimation of the IMT is provided with reference to the contour based model. Issue such as noise in ultrasound imaging, tracing of the IMT, methods of segmentation of the CCA pertaining to automation of the process and validation of such segmentation techniques are addressed in this work. Two inferences are derived from this study, first image descriptors such as SURF and MSER techniques provide a possible way to identify IMT from the given ultrasound images. The second finding illustrates the validation of such descriptors through machine learning techniques such as SVM based regression model.

REFERENCES

1. W. H. Organization, Prevention of cardiovascular disease. World Health Organization, 2007.
2. J. J. Badimon, B. Ibanez, and G. Cimmino, “Genesis and dynamics of atherosclerotic lesions: implications for early detection,” Cerebrovascular Diseases, vol. 27, no. Suppl. 1, pp. 38–47, 2009.
3. M. Walter, “Interrelationships among hdl metabolism, aging, and atherosclerosis,” Arteriosclerosis, thrombosis, and vascular biology, vol. 29, no. 9, pp. 1244–1250, 2009.
4. A.-M. Kampoli, D. Tousoulis, C. Antoniades, G. Siasos, and C. Stefanadis, “Biomarkers of premature atherosclerosis,” Trends in molecular medicine, vol. 15, no. 7, pp. 323–332, 2009.
5. F. Destrempes, J. Meunier, M.-F. Giroux, G. Soulez, and G. Cloutier, “Segmentation in ultrasonic b-mode images of healthy carotid arteries using mixtures of nakagami distributions and stochastic optimization,” IEEE Transactions on Medical Imaging, vol. 28, no. 2, pp. 215–229, 2008.
6. S. Golemati, J. Stoitsis, T. Balkizas, and K. Nikita, “Comparison of b-mode, m-mode and hough transform methods for measurement of arterial diastolic and systolic diameters,” in 2005 IEEE Engineering in Medicine and Biology 27th Annual Conference, pp. 1758–1761, IEEE, 2006.
7. P.-J. Touboul, M. Hennerici, S. Meairs, H. Adams, P. AmarencN. Bornstein, L. Csiba, M. Desvarieux, S. Ebrahim, M. Fatar, et al., “Mannheim carotid intima-media thickness consensus (2004–2006),” Cerebrovascular diseases, vol. 23, no. 1, pp. 75–80, 2007.
8. P. Pignoli and T. Longo, “Evaluation of atherosclerosis with b-mode ultrasound imaging.,” The Journal of nuclear medicine and allied sciences, vol. 32, no. 3, pp. 166–173, 1988.
9. Liguori, A. Paolillo, and A. Pietrosanto, “An automatic measurement system for the evaluation of carotid intima-media thickness,” IEEE Transactions on instrumentation and measurement, vol. 50, no. 6, pp. 1684–1691, 2001.
10. J. H. Stein, C. E. Korcarz, M. E. Mays, P. S. Douglas, M. Palta, H. Zhang, T. LeCaire, D. Paine, D. Gustafson, and L. Fan, “A semiautomated ultrasound border detection program that facilitates clinical measurement of ultrasound carotid intima-media thickness,” Journal of the American Society of Echocardiography, vol. 18, no. 3, pp. 244–251, 2005.
11. F. Faita, V. Gemignani, E. Bianchini, C. Giannarelli, L. Ghiadoni, and M. Demi, “Real-time measurement system for evaluation of the carotid intima-media thickness with a robust edge operator,” Journal of ultrasound in medicine, vol. 27, no. 9, pp. 1353–1361, 2008.
12. Schmidt and I. Wendelhag, “How can the variability in ultrasound measurement of intima-media thickness be reduced? studies of interobserver variability in carotid and femoral arteries.,” Clinical physiology (Oxford, England), vol. 19, no. 1, pp. 45–55, 1999.
13. Q. Liang, I. Wendelhag, J. Wikstrand, and T. Gustavsson, “A multiscale dynamic programming procedure for boundary detection in ultrasonic artery images,” IEEE Transactions on medical imaging, vol. 19, no. 2, pp. 127–142, 2000.
14. M. A. Gutierrez, P. E. Pilon, S. Lage, L. Kopel, R. Carvalho, and S. Furuie, “Automatic measurement of carotid diameter and wall thickness in ultrasound images,” in Computers in Cardiology, pp. 359–362, IEEE, 2002.
15. S. Lobregt and M. A. Viergever, “A discrete dynamic contour model,” IEEE transactions on medical imaging, vol. 14, no. 1, pp. 12–24, 1995.
16. C. P. Loizou, C. S. Pattichis, M. Pantziaris, T. Tyllis, and A. Nicolaides, “Snakes based segmentation of the common carotid artery intima media,” Medical & biological

engineering & computing, vol. 45, no. 1, pp. 35–49, 2007.

17. J. Alam, M. Hassan, A. Khan, and A. Chaudhry, “Robust fuzzy rbf network based image segmentation and intelligent decision making system for carotid artery ultrasound images,” Neurocomputing, vol. 151, pp. 745–755, 2015.
18. Kyriacou and C. Loizou, “Cardiovascular disease stratification based on ultrasound images of the carotid artery,” in Advanced Computational Intelligence in Healthcare-7, pp. 103–119, Springer, 2020.
19. L. Pedraza, C. Vargas, F. Narv´aez, O. Dur´an, E. Mu˜noz, and E. Romero, “An open access thyroid ultrasound image database,” in 10th International Symposium on Medical Information Processing and Analysis, vol. 9287, p. 92870W, International Society for Optics and Photonics, 2015.
20. Z. Hosseini and M. H. Bibalan, “B-mode ultrasonic images quality enhancement using an intelligent 5 5 pixels window averaging,” in 2018 8th Conference of AI & Robotics and 10th RoboCup Iranopen International Symposium (IRANOPEN), pp. 81–87, IEEE, 2018.
21. M. Cecelja, R. Sriswan, B. Kulkarni, S. Kinra, and D. Nitsch, “Association of pulse wave velocity and intima-media thickness with cardiovascular risk factors in young adults,” The Journal of Clinical Hypertension, vol. 22, no. 2, pp. 174–184, 2020.